DOI: 10.13009/EUCASS2023-447
Aerospace Europe Conference 2023 – 10TH EUCASS – 9TH CEAS

Design and Testing of a Reefed Disk-Gap-Band Parachute of Huygens Heritage for Sounding Rocket Recovery

Sahir Sujahudeen[⋆†], *Claudio Rapisarda*[⋆], *Thomas Mueller*[⋆], *Nachiket Dighe*[⋆] *and Erwin Mooij*[⋆]
[⋆]*Faculty of Aerospace Engineering, Delft University of Technology*
Kluywerweg 1, 2629 HS. Delft, The Netherlands
M.S.Sujahudeen@student.tudelft.nl C.Rapisarda@student.tudelft.nl T.H.Muller@student.tudelft.nl
N.P.Dighe@student.tudelft.nl E.Mooij@tudelft.nl
[†]Corresponding author

Abstract

This paper presents the development of a reefed Disk-Gap-Band (DGB) parachute with Huygens heritage for sounding rocket recovery. It starts with an overview of the rocket mission and then discusses the DGB design and geometric parameters. The integration of skirt reefing to minimize shock loads during inflation is explained. System verification tests, specifically tensile tests, are described. Wind tunnel testing was performed on a scaled-down version of the parachute with an active reefing system, yielding valuable information on drag and reefing performance. The paper concludes with recommendations for future DGB development.

Nomenclature

α	Geometric Suspension Angle (deg)	G	Gravity Force (N)
λ_g	Geometric Porosity (-)	H_b	Band Height (m)
ψ	Geometric Reefing Angle (deg)	H_g	Gap Height (m)
τ	Reefing Line Ratio (–)	L_{sus}	Suspension Line Length (m)
θ	Angle of Oscillation (deg)	N_{sus}	Number of Suspension Lines (–)
D_c	Disk Diameter (m)	S_0	Nominal Area (m^2)
D_p	Projected Diameter (m)	SF	Safety Factor (–)
D_v	Vent Diameter (m)	T	Tensile Force (N)
D_0	Nominal Diameter (m)	T_{cl}	Cloth Tension (N)
D_{max}	Maximum Drag (N)	T_{reef}	Reefing Tension (N)
F_{riser}	Riser Force (N)		

1. Introduction

Sounding rockets are widely employed across numerous scientific and engineering disciplines for data gathering, research, and technology demonstration. Their advantages, such as greater flexibility and enhanced accessibility to specific atmospheric and microgravity regions, make them compelling vehicles of significant interest. In line with the growing emphasis on sustainability and cost-effectiveness, the development of recovery systems for this class of rockets has gained great importance. While reusability and cost-reduction are primary drivers, many other reasons support the pursuit of recovery for rocket hardware including payload retrieval, post-flight analysis and safety requirements on the landing location of the launcher's parts.[11]

With the goal of addressing the need for recovery systems, The Parachute Research Group (PRG) within the Delft Aerospace Rocket Engineering (DARE) at Delft University of Technology (TUD) has developed several recovery technologies over the years. The Supersized Parachute-Enabled Atmospheric Re-entry mission (SPEAR II) mission, amongst the projects devised in PRG, aims to develop a parachute system for sounding rocket components weighing up

DOI: 10.13009/EUCASS2023-447

to 90 kg. The paper details the design, manufacturing and wind-tunnel testing of the Disk-Gap-Band (DGB) parachute conducted within the SPEAR II project. A rendering of the parachute presented in this work is shown in Figure 1.

DGB parachutes have been the predominant choice for deceleration from supersonic to subsonic speeds since the Viking missions in 1976. Initially developed for high-altitude meteorological rocket applications in the late 1960s[2] and later chosen for the successful PEPP program conducted by NASA in the 1970s, the DGB's sustained popularity is attributed to its heritage and reliable performance.[19] The choice of the parachute type is motivated by its favorable balance between drag and stability coupled with its ease of manufacturing and low packing volume. Thanks to its simple design consisting of a planar canopy disk with a cylindrical band of material secured to rigging lines, the parachute is easily tested at a small scale in wind tunnels.[17]

Two distinguished types of DGB designs are identified as the most well-established in the literature, namely the Viking design and the one developed for the ESA Huygens mission.[19] While numerous configurations were derived from the Viking design, the distinctive characteristic was the doubled gap height in Huygens DGB compared to Viking's derivatives. This modification notably contributed to improved stability.[10] Because of this improved performance, which is desirable for sounding rocket recovery applications, the Huygens DGB design heritage is explored to size the parachute described in this work.

The heritage of this parachute type is firmly established because of the comprehensive database of aerodynamic data gathered through Earth-based supersonic testing, ground-based wind tunnel tests and low-altitude drop tests which have been conducted in supersonic conditions.[2] An example is given by the Huygens heritage DGB flown onboard the MAXUS-9 sounding rocket.[8] Nevertheless, scarcer aerodynamic data is available in the literature for subsonic conditions. Following the program sponsored by ESA in 2015 to investigate alternative subsonic parachutes,[18] subsonic data were gathered by Underwood et al.[19] through free-flight and wind tunnel testing in support of the earlier wind tunnel campaign.[20] However, a discrepancy larger than 50% in drag coefficient was yielded between such tests, suggesting the need for further studies.

In line with the mission objective of scaling a parachute for heavier payloads, in addition to expanding the available aerodynamic database of Huygens-like decelerators, the effect of reefing is also addressed in this research. Defined as the ability to reduce the diameter and surface area of a parachute in flight, the reefing capability not only offers improved control of the descent rate and reduced lateral velocities at high altitudes but also lowers the opening loads experienced by the decelerator when actuated during deployment.[6] Active skirt reefing, which is the conventional type of reefing where the leading edge of the band is constrained from fully inflating by a cord, has already been investigated for DGB parachutes in supersonic conditions.[14,21] Various undesired behaviors were observed as a result of reefing such as erratic dynamics and violent instabilities.[1,21] However, active skirt reefing has never been investigated for DGB deployment in subsonic conditions.

Drawing from these considerations, this work aims to address manifold objectives in the field of sounding rocket retrieval by focusing on the design of a DGB with active skirt reefing, inspired by the legacy of the Huygens parachute. The primary goal of the research is to propose a scaled version of the Huygens decelerator to enable the controlled descent and retrieval of sounding rocket hardware. The cost-effective manufacturing techniques implemented and described in this work maintain high standards of performance and reliability while accounting for limited testing opportunities. The novel contributions of this paper include the discussion and assessment of the aerodynamic test data gathered in the Open Jet Facility (OJF) at the TUD in the subsonic regime with and without active skirt reefing. The investigation of the drag performance and reefing performance of the proposed DGB design not only complement and extend the scarce aerodynamic data retrieved in the literature but are also paramount to providing insights into the development and future improvement of recovery systems for sounding rockets. By facilitating the recovery and reuse of rocket components, this research promotes sustainable development goals, thereby minimizing resource consumption.

Having contextualized the need and objectives of this work in Sec. 1, an overview of the mission used to define the recovery system requirements is outlined in Sec. 2. The design methodology of the parachute is described in Sec. 3, where the geometry and dimensions of the full-scale and test-model DGB are established. The design methodology is extended onto Sec. 4 to illustrate the approach taken to select and size the type of reefing to be applied to the DGB parachute. Section 5 illustrates the materials used to manufacture the parachute and delineates the cost-effective production strategies adopted. The main results of the paper are presented in Sec. 6, consisting of the set-up and experimental measurements obtained from the tensile testing and wind-tunnel testing campaigns. The conclusions are drawn in Sec. 7, where recommendations are provided for further research.

2. Mission Overview

Driven by the primary goal of reusability, the SPEAR II project aims to design, manufacture and test a medium-sized recovery system capable of safely landing the heavier parts of sounding rockets, or even the entirety of the vehicle. As the decision to recover heavy hardware has a significant effect on the recovery system design, a reference mission is

DOI: 10.13009/EUCASS2023-447

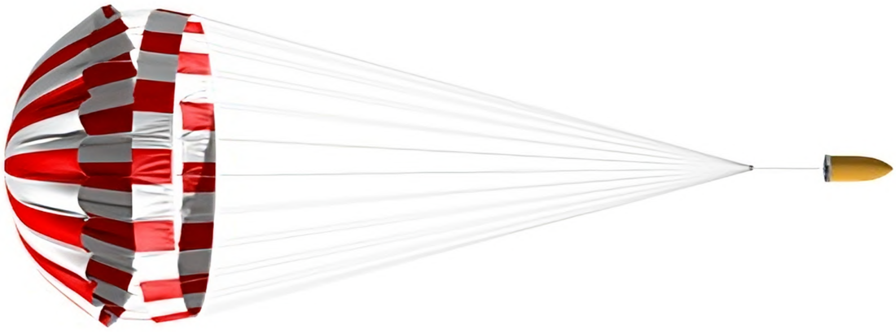

Figure 1: Rendering of the unreefed Huygens-heritage DGB parachute attached to sounding rocket nosecone

Table 1: Sounding rocket mass breakdown; Adapted from Pepermans et al.[11]

Vehicle	Manufacturer	Apogee (km)	Post-Separation Mass Ratio (-)	Total Dry Mass (kg)	Total Wet Mass (kg)
Stratos II+	DARE	50	15 : 60	75	185
Stratos III	DARE	80	15 : 90	105	330
Stratos IV	DARE	100+	15 : 87	102	328
Stratos V	DARE	26	1 : 1	125	213
CanSat v7	DARE	1	0.5 : 11.5	12	16
REXUS 4[15]	REXUS/BEXUS	175	152 : 400 (111) + 598	Unknown	1175.3
Heros 3[7]	HyEnD	32.3	Na : Na	75	161
Nexo II[16]	CopSub	12.6	5.9 : 172.1	178	292

required to define the system requirements. The 4th generation of the Stratos sounding-rocket family was designed and manufactured by DARE to reach and surpass the boundary of space.[12] The Stratos IV booster mass, equivalent to 90 kg, is used as payload mass as it is representative of the dry mass of the sounding rocket parts developed within DARE and beyond, as listed in Table 1.

Because of its ambitious mission, Stratos IV represents a challenging yet suitable application study for sounding rocket retrieval. Based on six-degree-of-freedom two-body system simulations, the ballistic re-entry trajectory of the Stratos IV booster configuration with a main parachute was evaluated with an initial horizontal velocity of 500 m/s at an apogee of 160 km and an average nosecone drag coefficient of 2.8. Attaining a deployment dynamic pressure of 4.5 kPa at Mach 0.35 by imposing a subsonic deployment as shown in Figure 2, the parachute is sized to ensure a terminal velocity of 20 m/s for a safe water landing. A minimum nominal area of 7.7 m^2 is therefore required by assuming a drag coefficient of 0.5, common as the lower end drag performance of Huygens DGBs,[19,20] though a more conservative value of 8 m^2 is chosen. The application of the proposed main parachute to a potential mission is shown in Figure 3 for a two-stage recovery system.

3. Parachute Design

To begin the design process for a recovery system with a conservative nominal area of 8 m^2, it is first crucial to select the type of parachute. Initially, various parachute types were considered, including solid parachutes. However, these decelerators exhibit drawbacks, such as high opening forces and low stability.[6] On the other hand, annular parachutes offer excellent drag and stability. However, they face challenges when it comes to supersonic regimes. Meanwhile, cruciform parachutes provide good stability, satisfactory drag performance, and low opening forces. Nevertheless, their performance in supersonic regimes is unproven. In contrast, the conical ribbon parachute excels in supersonic inflation and stability. However, building scale models of this type can be challenging.[6] In contrast, DGB parachutes demonstrate higher packing efficiencies, requiring less volume. Moreover, they are easy to manufacture due to their simpler structure, consisting of fewer parts compared to conical ribbons. Therefore, the DGB parachutes emerge as the preferred choice for the sounding rocket recovery system

DOI: 10.13009/EUCASS2023-447

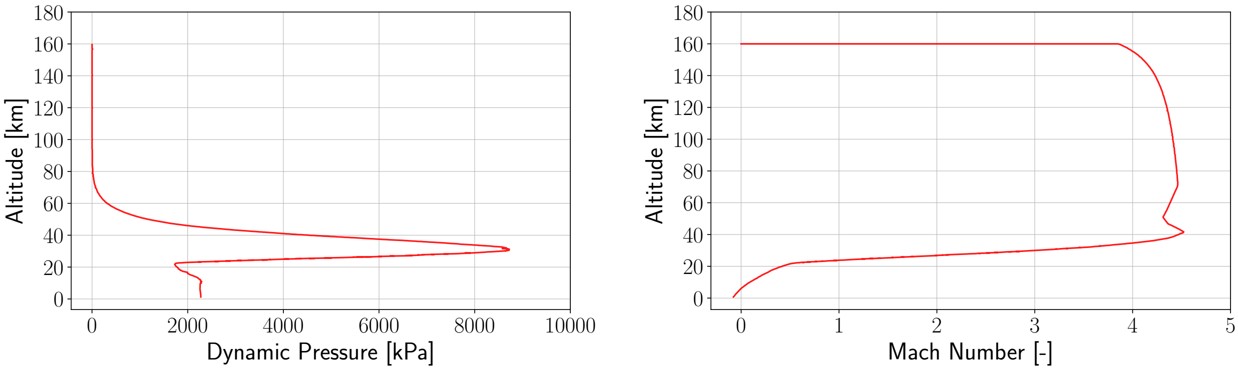

(a) Altitude vs. Dynamic Pressure

(b) Mach vs. Altitude

Figure 2: Simulated dynamic pressure and Mach number with altitude for a Stratos IV Booster recovery mission

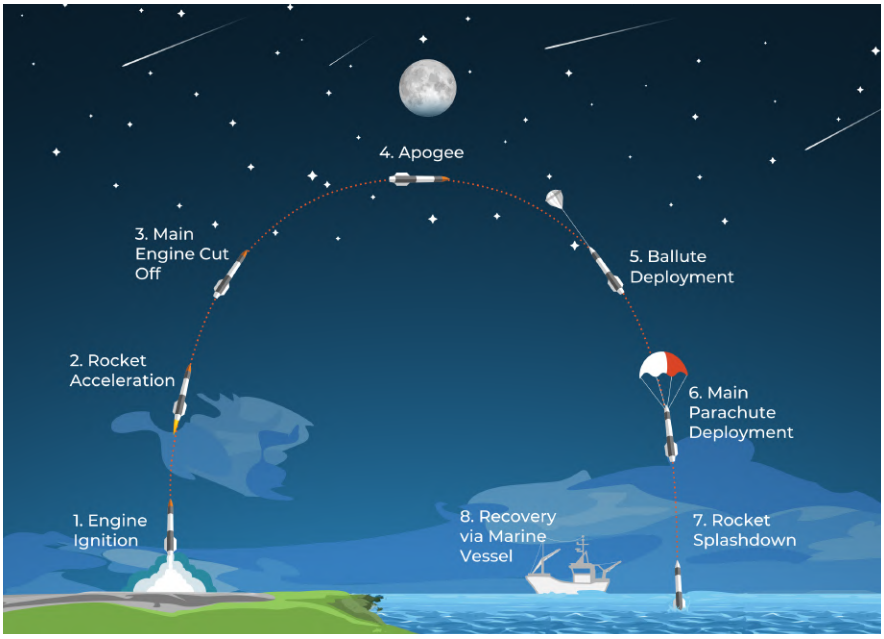

Figure 3: Concept of operations of the proposed recovery system

3.1 Disk Gap Band Design

The disk gap band was designed as a result of an effort to create a parachute with reliable openings in low-density environments, featuring good drag and stability characteristics, simple construction, and low packing volume. To give the parachute the required stability, a gap was introduced to provide the geometric porosity in the canopy. The resulting DGB parachute, illustrated in Figure 4 with its major components, has undergone iterative design improvements.[2]

Three significant DGB variations exist: the original Viking parachute, built with a geometric porosity of 12.5%; the modified Viking DGB for the MER and Pathfinder missions, which has a doubled band length and, therefore, a geometric porosity of approximately 9.3%; and the Huygens mission DGB, which features a doubled gap length compared to the Vikings DGB, leading to a geometric porosity of around 22.4%. Both modifications were made to improve the stability of the angle of oscillation to a 3σ value of less than 15°, albeit at the cost of worse drag performance. In contrast, Mars Phoenix and MSL employed a direct Viking-type parachute as they required more drag than stability.

The DGB parachutes are sized using non-dimensional ratios, as shown in Table 2. The gores can then be sized as illustrated in Figure 5. Although information about the Viking DGB and Pathfinder DGB are widely accessible, comprehensive information on the Huygens DGB is not readily available. Therefore, approximations based on known sizes of a single parachute gore and band were employed to determine its ratios.

DOI: 10.13009/EUCASS2023-447

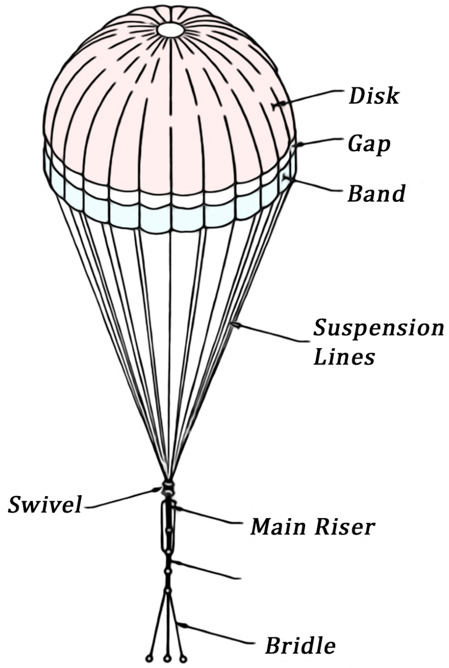

Figure 4: Overview of DGB design elements

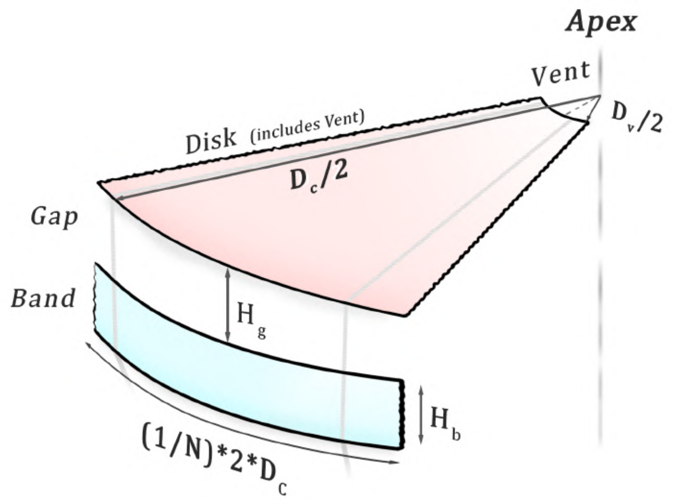

Figure 5: Overview of parachute nomenclature used for DGB parachute gore

Table 2: Summary of the Viking, Pathfinder and Huygens DGB geometry compared to present work. The information is derived from a historical summary by the Jet Propulsion Laboratory[2] and a parachute seminar by Vorticity.[20]

Parameter	Viking	Pathfinder	Huygens	Present Work
Nominal Diameter, D_0 (m)	D_0	D_0	D_0	D_0
Nominal Area, S_0 (m^2)	$0.25\pi D_0^2$	$0.25\pi D_0^2$	$0.25\pi D_0^2$	$0.25\pi D_0^2$
Geometric Porosity, λ_g (-)	$0.125S_0$	$0.093S_0$	$0.224S_0$	$0.224S_0$
Vent Diameter, D_v (m)	$0.07D_0$	$0.063D_0$	$0.099D_0$	$0.048D_0$
Disk Diameter, D_c (m)	$0.720D_0$	$0.624D_0$	$0.686D_0$	$0.686D_0$
Gap Height, H_g (m)	$0.042\ D_0$	$0.036D_0$	$0.0775D_0$	$0.080D_0$
Band Height, H_b (m)	$0.121D_0$	$0.233D_0$	$0.113D_0$	$0.113D_0$
Suspension Line Length, L_{sus} (m)	$1.7D_0$	$1.7D_0$	$2.0D_0$	$2.0D_0$

The present work describes the final geometry of the DGB parachute in this paper, which closely follows the ratios of the Huygens parachute. A notable difference lies in the vent diameter and band height. This variation is a deliberate choice to trade vent area for gap area while maintaining a geometric porosity of 22.4%. The intention behind this trade-off was to introduce a new data point within the Huygens design.

The decision to prioritize the Huygens parachute over the Viking heritage parachute was primarily motivated by the significant research value associated with the Huygens design and the limited availability of data points. Furthermore, the antiquity of the Viking design played a role, as advancements in parachute technology and improved understanding of aerodynamic principles have emerged since the development of the Viking design. To determine the number of suspension lines needed for the parachute design, the following free-body diagram considers a scenario where the vehicle is free-falling towards the ground while experiencing oscillations due to instability or external gusts. In this situation, one suspension line is exposed to the highest load. Accounting for this scenario and adding a safety margin ensures a safe design.

In the case of the oscillatory scenario, a more comprehensive force equilibrium analysis is required, as depicted in Figure 6. To determine ΔT, the drag force D and lift force L need to be quantified. Therefore, a simple force balance would result in too many unknowns that would require assumptions. To address this problem more accurately, a moment equilibrium can be established around the point where D and L are zero. By doing so, the moment exerted by D and L becomes negligible and does not contribute to subsequent equations. This approach effectively reduces the unknowns to only T, ΔT, and G as the relevant components in the analysis. By establishing a moment equilibrium around the aforementioned point, considering the decomposition of forces in the directions perpendicular and parallel

DOI: 10.13009/EUCASS2023-447

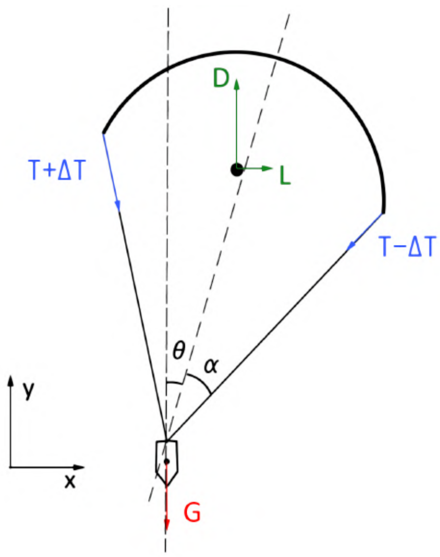

Figure 6: Parachute-forebody force balance diagram

to the riser, the following moment equation is derived:

$$\Sigma M = [(T + \Delta T) - (T - \Delta T)] \cos\alpha \frac{D_p}{2} = L_{sus} G \cos\alpha \sin\theta \rightarrow \Delta T = \frac{G L_{sus} \sin\theta}{D_p} \tag{1}$$

where D_p is the projected diameter, α is the geometric angle the suspension line forms to the mid line, θ is the angle of oscillation. Therefore, the total tension is:

$$T = \frac{D_{\mathrm{max}}}{N_{\mathrm{sus}} \cos\alpha} + \frac{G L_{\mathrm{sus}} \sin\theta}{D_{\mathrm{p}}} \rightarrow N_{\mathrm{sus}} = \frac{D_{\mathrm{max}}}{\left(\frac{T}{SF} - \frac{G L_{\mathrm{sus}} \sin\theta}{D_{\mathrm{p}}}\right) \cos\alpha}, \qquad \alpha = \sin^{-1}\left(\frac{D_p}{2 L_{sus}}\right) \tag{2}$$

where D_{max} is the maximal drag force, N_{sus} is the number of suspension lines, T represents the maximum tensile force that the suspension line can sustain and SF denotes the applied safety factor to this tensile force. (2) allows for a conservative estimation of the number of suspension lines, particularly in extreme scenarios. Consequently, the number of gores can be deduced as it must align with the number of suspension lines. The angle α is therefore determined geometrically.

The expected maximum drag and gravity force G follow from the mission overview in Section 2 and equal 18000 N from drag and 882.9 N from gravity. To incorporate the opening force, a safety factor must be applied. According to Knacke,[6] DGB parachutes typically require a safety factor of 1.3. Therefore, the resulting maximum drag force denoted as D_{max}, amounts to 23400 N. Safety Factors SF for suspension lines range from 1.9 for the Viking mission to 2.31 for MER.[2] Thus, a SF of 2.25 is chosen in the present work. Huygens DGB parachutes are typically stable at incidences below 10°.[18] To that end, θ was selected to be 10°. The tensile force stems from the Spectra 725 lbf used for testing. The projected diameter D_p is calculated from the sizing ratio for the disk diameter D_c given in Table 2 for a nominal area S_0 of 8 m^2. In reality, D_p will be smaller than D_c making this a conservative estimate. This information and the final number of suspension lines N_{sus} is given in Table 3. The geometry of the gores of the parachute is defined and calculated as illustrated in Figure 5.

The final geometry of the full-scale design intended for the SPEAR II mission is presented in Table 4. This design incorporates the sizing ratios from Table 2 and the calculated number of suspension lines from Table 3. Furthermore, scaled-down versions of the full-scale parachute were created for wind tunnel testing. The scaling was carefully executed to ensure compatibility with the available wind tunnel facility, which has a test area of 2.85 m x 2.85 m. However, it is worth noting that the manufactured test model turned out to be smaller than the intended design due to the expertise of the manufacturing operators.

DOI: 10.13009/EUCASS2023-447

Table 3: Parachute Design Parameters

Parameter	Symbol	Value	Unit
Maximum Drag	D_{max}	23400	N
Tensile Force	T	725	lbf
Geometric Suspension Angle	α	9.73	deg
Angle of Oscillation	θ	10	deg
Safety Factor	SF	2.25	–
Gravity Force	G	882.9	N
Suspension Line Length	L_{sus}	6.48	m
Projected Diameter	Dp	2.19	m
Number of Suspension Lines	N_{sus}	24	–

Table 4: Geometrical DGB Dimensions

Parameter	Full-Scale Design	Test-Model Design	Manufactured Test-Model	Units
Nominal Diameter, D_0	3.190	1.514	1.418	m
Nominal Area, S_0	8.00	1.80	1.58	m^2
Geometric Porosity, λ_g	22.4	22.4	22.8	%
Vent Diameter, D_v	0.152	0.072	0.073	m
Disk Diameter, D_c	2.190	1.039	0.960	m
Gap Height, H_g	0.255	0.121	0.118	m
Band Height, H_b	0.360	0.171	0.165	m
Suspension Line Length, L_{sus}	6.38	3.0	3.0	m
Suspension Line Number, N_{sus}	24	12	12	-

4. Reefing Design

Parachute reefing is a widely used in recovery systems to reduce the maximum loads experienced by the parachute during inflation. For when the target deployment envelopes incur loads that are too extreme to be withstood by the structural elements of the parachute, a reefing system can be used as a tool in susceptible points of failure within the parachute complex. Performing research and implementation of the concept would be useful to increase the versatility and endurance of the explored DGB design and further expand the capabilities of existing recovery technology in DARE. Furthermore, the limited information on its application to subsonic-deployed DGBs motivates it as a point of research.

For the parachute being developed, active skirt reefing at the bottom of the disk was chosen over other methods. The alternative, passive methods are not used in high load reduction scenarios and lack controllability. In addition, skirt reefing has been and is still extensively used in entry, descent, and landing of manned and unmanned missions, however integration into DGBs remains limited. A flight test performed by Langley Research Center[14] demonstrated the applicability on a Viking-based DGB and was largely used as reference for the design of the in-house reefing system. The test DGB of 12.2m nominal diameter was reefed to a reefing line ratio τ of 28%, with a steady-state drag area ratio of 0.526. Based on this data point, it was decided to further investigate the load reductions with lower τ (<20%) to reduce the structural criticality of the components used for active skirt reefing and the parachute riser.

An important design factor when implementing skirt reefing is the tension experienced by the reefing line. To this end, Potvin and Patel[13] provide a simplified, analytical method to evaluate an upper bound for very low-porosity parachutes. Under the assumptions of the parachute complex having a single confluence point, low line ratios, and the disk conforming to a spherical shape when reefed; the upper bound for line tension T_{reef} to the riser force F_{riser} (force ratio) can be formulated by Equation (3) for a given reefing line ratio τ. The parameters present disk gap band in Table 2 and reefing line ratios below 30% lead to a force ratio of about 0.25. Note that F_{riser} represents the maximum load experienced during parachute operation and the selected reefing line's breaking strength should encompass a specified safety factor.

$$\frac{T_{reef}}{F_{riser}} < \frac{1}{4}\left[1-\left(\tau\frac{D_c}{2L_{sus}}\right)\right] \tag{3}$$

DOI: 10.13009/EUCASS2023-447

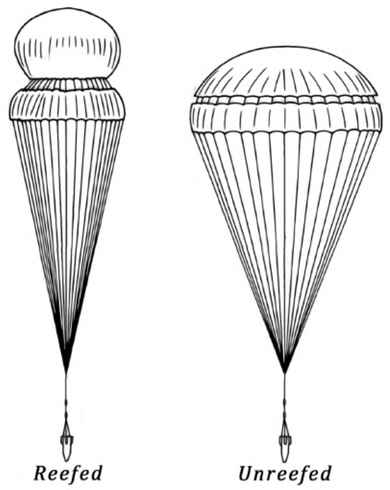

Figure 7: Skirt reefing visualized in a DGB, in reefed and unreefed states[14]

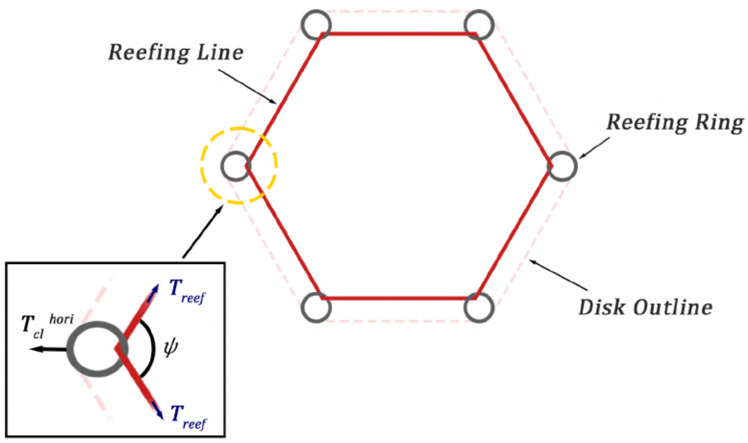

Figure 8: Bottom-up view of a reefed canopy, illustrating the routing of the reefing line through reefing rings

Figure 8 illustrates the manner in which reefing rings are attached to the hem of the disk, constricting the parachute to the reefing line diameter. The radial force experienced by each ring - for a design with one ring per gore - can be found using Potvin and Patel,[13] with (4) and the force overview presented in Figure 8.

$$T_{cl} = 2T_{reef}\sin\psi, \qquad \text{with} \quad \psi = \pi - \frac{2\pi}{N_{sus}} \tag{4}$$

5. Materials and Manufacturing

Material and manufacturing considerations of a reefed DGB were treated simultaneously with the structural design of the decelerator. Decelerators need to withstand the shock loads during deployment and intensive heat at high dynamic pressures, but also need to fit into the rocket at minimal mass. Therefore, canopy, suspension lines and riser-bridle materials strive for high UTS/E-modulus whilst maintaining low specific mass/cost of acquisition.

The canopy must be able to withstand inflation loads and be resistant to fracture propagation when encountering snag hazards. Generous material porosity is desired to complement the high geometric porosity of a DGB. Therefore, F-111 ripstop nylon is chosen as the canopy material. With a temperature resistance of approximately 60°, nylon provides the basis for thermal resistance under high dynamic pressures. A 40-denier Nylon 6 weave,[9] boasts a tensile strength of 11.6 N/mm^2 and a tear strength of 49.8 kN/m. Considering the anisotropic nature of nylon, which is addressed in the next section as shown in Figure 11a for different fiber orientations, the nylon fibers should generally be aligned in the load-carrying direction, in the tangential direction to the DGB contour. Small misalignments in sewing are inconsequential.

The individual canopies of the 'disk' and 'band' need to be stitched together in a gore assembly (Figure 11a). Canopy attachment significantly reduces strength. A preliminary strength reduction factor of 0.5 can be assumed based on tensile test data. Further sample tests were conducted to understand the effect of sewing patterns, reinforcement tape material, and width on tensile strength (Figure 11b). Aramid tape with a width of 25mm, sewn with a straight stitch, appears to be the strongest choice for canopy attachment. Alternatively, a zig-zag stitch can be used, although it provides less strength. To maximize overlap, a felled seam is recommended. In a DGB parachute, the reinforcement tape also serves as a connector between the disc and the gap, as illustrated in Figure 4, promoting a continuous and uninterrupted load path within the parachute. The overall strength of the gores allows for the attachment of the reefing system near the skirt through bolts (Figure 12a). Additionally, high-stress concentrations are expected near the vent region,[5] suggesting the incorporation of tape around the vent hole. It is specified that the majority of the load is carried by the reinforcement tape.[4] An optimally designed gore can be utilized by reducing the surface density of the canopy fabric, allowing the fabric to primarily serve an aerodynamic function in maintaining shape and stability, while thicker reinforcement tape retains structural integrity. Further tensile tests can be conducted using various fabric and reinforcement tape thickness combinations to better understand failure characteristics.

The gore assembly for a parachute should be compatible with the lines connecting it to the recovery vehicle. Suspension lines should occupy minimal volume while maintaining sufficient strength and stiffness. Practical consid-

DOI: 10.13009/EUCASS2023-447

erations and ease of acquisition apply. The two main line connection mechanisms are knots and splices. Splices offer high repeatability in line lengths, unlike knots. Spectra 725 lbs is chosen as the suspension line material. Tensile testing, as shown in Figure 11, demonstrates the superior strength of splices compared to knots. Knots struggle to sustain loads above 2.5 kN, while splices fail at 3.1 kN (slightly below the ultimate tensile strength of Spectra 725 lbs at 3.28 kN).

The apex of all suspension lines attach to a riser, that in turn finally introduces the DGB to the recovery vehicle. The design of the riser is often pertinent to the maximum shock loads for a flight trajectory, rather than the decelerator itself. In any case, it is general to assume that risers withstand loads as extreme as 20-30kN.[12] There is no doubt that high performance (braided) rope such as that comprised aramid, Twaron® or Arabraid fibers is desired. The exact riser is highly dependent on acquisition at the time of fabrication.

Parachutes are Z-folded to mimic the elastic behavior of a spring during deployment. To reduce snag hazards, the DGB's components should be protected with a parachute bag. Tough, dry, waterproof fabric such as Paratex is desired. Such a pack-job has led to successful deployment during wind-tunnel tests described in Subsection 6.2. Extensive hydraulic/compression tests are suggested to optimize the pack-job for volume.

6. Parachute Testing

The experimental data collected throughout the research project is categorized into two major branches of parachute engineering. The first branch focuses on the materials utilized to manufacture the DGB parachute. To explore this aspect, a comprehensive tensile test campaign was carried out at the Delft Aerospace Structures and Materials Laboratory. The strain behavior of various canopy materials, reinforcement tapes, stitch types and suspension lines or risers has been recorded under increasing loading conditions. The second branch is concerned with the aerodynamic drag performance of the sub-scaled DGB which has been tested in the OJF wind tunnel at the High-Speed Laboratory of TUD.[3] The wind tunnel facility measures 13 meters in width and 8 meters in height, providing a 3:1 contraction rate. This configuration enables the testing of relatively large parachutes at maximum freestream speeds of around 35 m/s.

6.1 Parachute Material Tensile Testing

In order to verify the suitability of the selected materials for a sounding rocket recovery system, which must meet the requirements outlined in the preceding sections of this paper, a comprehensive tensile testing campaign was conducted. The primary objective was to evaluate the behavior of the parachute components under anticipated aerodynamic loading conditions and investigate their failure modes. Thus, all tests are conducted until failure of the test samples.

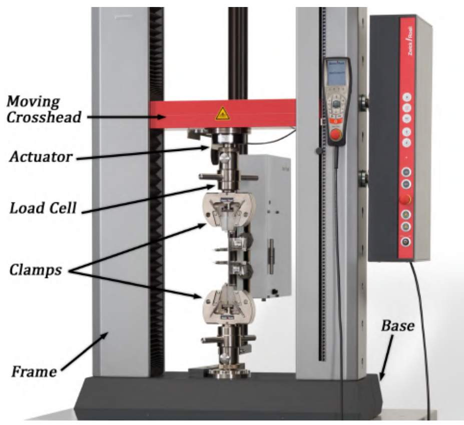

Figure 9: Experimental tensile test set-up[22]

Table 5: Parachute Material Tensile Test Matrix

Sample Type	Sample Material	Dimensions (mm)	Sample Type	Orientation (deg)
Canopy	Ripstop Nylon	50 × 80	Plain	0
Canopy	Ripstop Nylon	50 × 80	Plain	45
Canopy	Ripstop Nylon	50 × 80	Plain	90
Canopy	Ripstop Nylon	50 × 80	Nylon Tape	0
Gore	Ripstop Nylon	50 × 20	Straight Stitch	0
Gore	Ripstop Nylon	50 × 20	Zig-Zag Stitch	0
Gore	Aramid	50 × 20	Straight Stitch	0
Gore	Aramid	50 × 20	Zig-Zag Stitch	0
Gore	Aramid	25 × 20	Straight Stitch	0
Gore	Aramid	25 × 20	Zig-Zag Stitch	0
Line	Aramid	300	Perfection Knot	0
Line	Aramid	300	Double Bowline Knot	0
Line	Aramid	300	Poacher's Knot	0
Line	Spectra	300	Splice	0

The testing setup, as illustrated in Figure 9, involved a rectangular sample for the parachute fabric or straight strings for the suspension lines and risers, which are securely clamped at both ends using a hydraulic system at 60 bar in a Zwick Universal Testing Machine. The overview of the tested items is provided in Table 5, where three samples are tested for each scenario. To enhance the frictional grip on the samples, rubber sheets were placed at each end between the fabric and the clamps. This ensured a reliable connection between the fabric and the setup. To measure the response of each sample, a 20 kN load cell was employed. The load cell recorded the forces exerted by the samples

DOI: 10.13009/EUCASS2023-447

as the bottom clamp pulled away at a maximum velocity of 50 cm/min, replicating the shocks experienced during actual flight conditions. Furthermore, the fixture in the clamp is chosen to ensure a uniform load distribution across the material sample to prevent stress concentration across specific regions of the material sample, which would not be representative of the tensile properties of the parachute material under deployment and inflation.

6.1.1 Canopy Cloth Material

Since ripstop nylon F-111 is chosen as the canopy material, its tensile behavior is investigated at three different angular orientations with respect to the vertical clamp direction. Namely, the nominal orientation of 0° is complemented with 45° and 90°. This is done to obtain experimental values more representative of a flight, where the parachute oscillations coupled with crosswinds could vary the loading direction. The results, displayed in Figure 11a reveal the approximately linear elongation of the samples under loading for both the warp and weft directions until failure is reached. Interestingly, the yield strength of the samples in the 0° and 90° orientation is 2.57-2.38 times larger than the 45° case respectively.

These results suggest the suitability of F-111 nylon for canopy when subjected to load in the normal direction as opposed to shear one, confirming the orthotropic nature of the tested nylon fabric. The effects of nylon tape applied over the baseline 0° F-111 nylon sample is also examined to model the attachment of different canopy elements. On one hand, the additional material contribution is found to be detrimental to the structural behavior of the sample as it reduces its yield strength by 1.74 times, bringing its elastic limit to an end when subjected to a load of approximately 490 N. On the other hand, it increases its ductility by unveiling a larger plastic strain which is otherwise not visible in the absence of nylon tape. The discrepancy highlights the different material responses that must be accounted for in the design stages due to the inclusion of an assembly connection. Therefore, it was of interest to further study the effect of different gore attachments on the stiffness/strength of the parachute- as detailed in subsubsection 6.1.2.

6.1.2 Gore Attachment

The combination of reinforcement tape and stitch type has been investigated according to the test matrix tabulated in Table 5, where Nylon and Kevlar/Twaron are used for the reinforcement tape materials with straight and zig-zag stitched. Three tests are conducted for each combination of reinforcement tape and stitch type to minimize random and measurement errors. The resulting stress-strain curves for all the tested combinations are plotted in Figure 11b.

The material response is comparable for all tested samples, showing a non-linear elongation with increasing loading until failure is reached. Almost no plastic displacement is measured, due to the abrupt failure of the gore samples. While the effect of the stitch type appears to be almost negligible for the 50 mm aramid samples, a zig-zag stitch is preferred over a straight one from a tensile behavior standpoint of Nylon F-111 as it increases its failure load from 363 N to 481 N in addition to increasing its stiffness by approximately one third. An increase in stiffness of about 10% is also measured for the 25 mm aramid sample, although the straight stitch fails at 800 N, whereas the zig-zag sample at 738 N. Despite minor differences in failure loads, it is clear that a gore assembly causes a substantial reduction in strength as compared to canopy only. The most drastic loss of strength can be up-to a factor of 2.2, marginally higher than the 1.93 recommended by Knacke[6] for main parachute canopies.

It was further observed that gore failure was caused by Nylon F-111 tear-out, at the edge of the reinforced tape. As the reinforcement tape material is stiffer than canopy material, it is stipulated that the edge of the tape introduces a local stress concentration in the fabric. The effect of the stress concentration is exaggerated by assembly's eccentricity (overlap joint area tends to rotate as opposed to remaining aligned with the fabric) under tensile load. At the same time, it was confirmed that the stitch and tape material still remain intact at failure load. These observations are seen in Figure 10.

6.1.3 Line Configurations

In contrast to the canopy testing, the maximum strength of the suspension lines and riser ropes are available prior to testing, as they are provided by qualified manufacturers. However, attachment of these lines and ropes, either to the riser or canopy generally reduce their tensile strength. Line attachment is achieved by means of knots or splices. Modeling various types of line termination is too complex to provide accurate or reliable results. Therefore, the tensile behavior of aramid and spectra line configurations is simply tested according to Table 5.

The resulting force-strain diagram is shown in Figure 11c for the tested samples. The highly non-linear elastic response shows a much larger stiffness for the spliced spectra rope than for the knotted aramid lines. Interestingly, while the double bowline knot and perfection knot only vary the gradient of the curve, the Poacher's knot leads to an increase in the range of 22-37% in load required to reach the plastic regime.

DOI: 10.13009/EUCASS2023-447

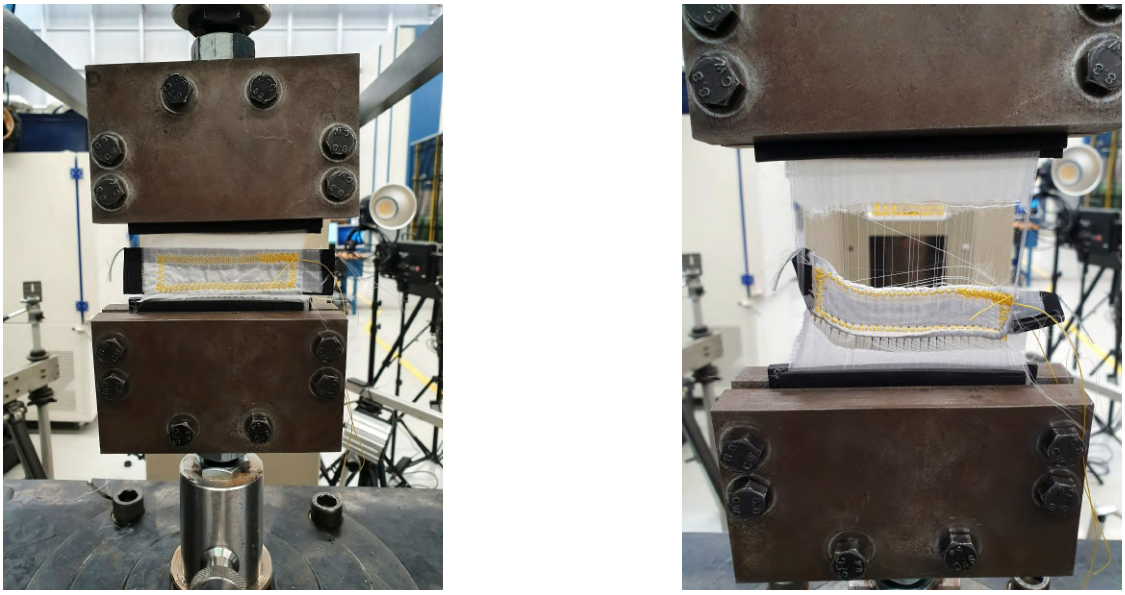

(a) Clamped sample material in pre-tension

(b) Gore sample material failure mode

Figure 10: Pre- and post- tensile test of Zig-zagged stitch ripstop nylon gore.

Further noting that Spectra 725 lbs (manufacturer rated) was used, the spliced configuration is measured to fail only at 3200 N (or 719 lbs). Such a high failure load value, almost as high as the manufacturer rating, confirms that a splice leads to negligible loss of tensile strength. Post-failure examination of the spectra lines revealed that line tear-out consistently occurred at the line's midpoint, and not at the location of the splice itself. All knotted samples, on the contrary, failed at the end of the knots. Perfection knots tend to get undone as it approaches ultimate tensile load whereas poacher's/double bowline break by over-tightening themselves. Although the exact sequence of events leading to the failure of a given knot is beyond the scope of the study, one can concluded that knot failure is highly local due to the presence of large stress concentrations. Since the knot fails significantly before the rope, it is verified that knots reduce tensile strength.

6.2 Subsonic Wind Tunnel Testing

The scaled-down parachute was tested in the closed-loop OJF windtunnel[3] in near-laminar subsonic flow conditions at nominal speeds between 10 m/s and 30 m/s with increments of approximately 5 m/s, at a room temperature environment and ambient air density of 1.17 kg/m^3. A tensile load sensor capable of measuring at 10^4 Hz was attached to the riser and measured the exerted drag force of the parachute. From in-house historical data on parachute testing at the OJF wind-tunnel, a calculated blockage factor of 10% for the unreefed test parachute was deemed within bounds to consider wall-interference effects as negligible.

Figure 12a and Figure 12b illustrate the parachute when active reefing is applied at the deployment. Notable are the visible skirt reefing line and the canopy constriction. Notice that the majority of the canopy constricted is caused by the disc, as opposed to the band. Two black boxes, visible on the skirt in Figure 12a, contain independent reefing systems. Specifically, each black box contains a custom wire cutter, pyro-technically actuated by a pre-programmed timer. Afterwards, these wire cutters cut the skirt reefing line to fully inflate the parachute. Although one reefing box is adequate for dis-reefing, a second one is included for redundancy.

The fully inflated chute is visible in Figure 13a and Figure 13b. The measured drag force is plotted in Figure 14 for the considered scenarios, where a digital Savitzky-Golay filter is applied to smooth the load cell data.

The aerodynamic performance of the unreefed parachute, plotted in Figure 14a unveils a steady-state drag coefficient between 0.54-0.57 when the drag area is taken to equal the nominal area of the manufactured sub-scale model in Table 4. The range of values shows an excellent agreement with the experimental data retrieved from the literature. Underwood et al.[19] indicate a drag coefficient of 0.49 for an incident test and 0.50 for a free flight test with an inflation time of 2.90 s. At the same time, Underwood and Sinclair[20] also present a corrected drag coefficient of 0.54-0.55 in a wind tunnel campaign at Mach 0.05. The consistent agreement with independent work validates the correct design methodology and manufacturing processes discussed in this work.

Following the verification of the steady-state behavior of an unreefed DGB, reefing (active and non-active) were

DOI: 10.13009/EUCASS2023-447

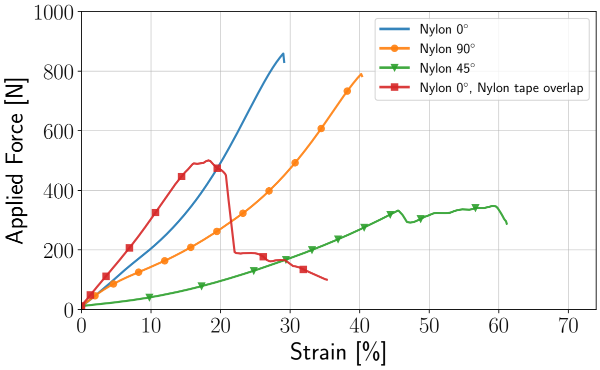

(a) Parachute Canopy Material

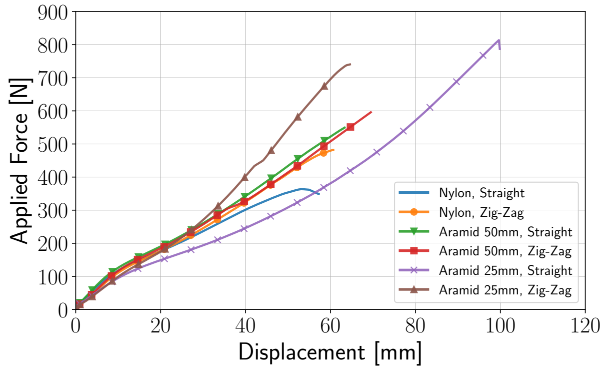

(b) Parachute Gores and Stitches

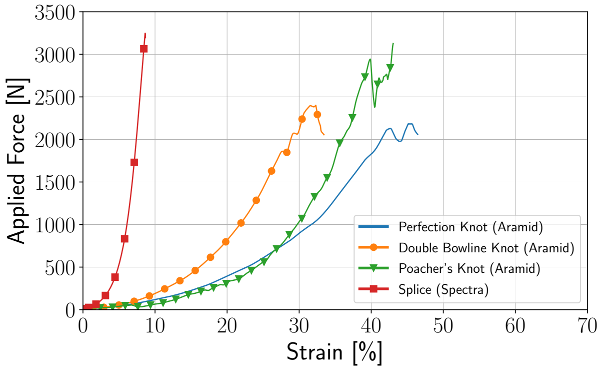

(c) Parachute Line Knots and Splices

Figure 11: Experimental Force-Strain curves obtained via tensile testing

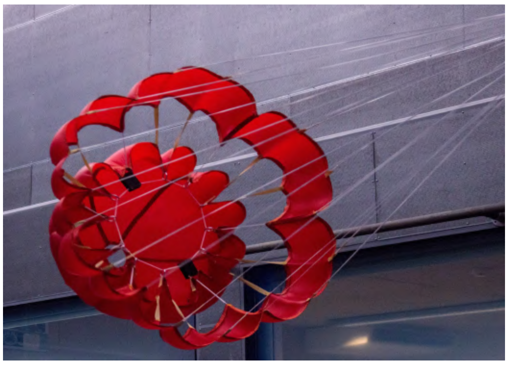

(a) Isometric view: two reefing boxes and skirt line visible

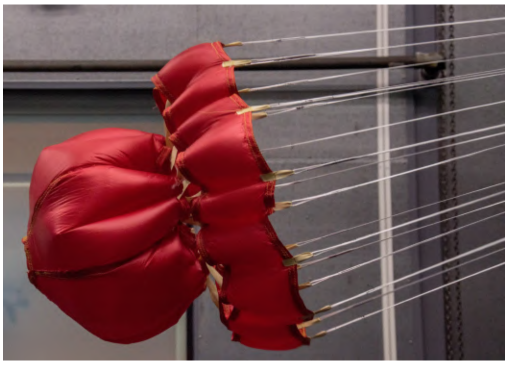

(b) Side view: canopy constriction at disk hem visible

Figure 12: Reefed DGB in OJF Windtunnel

investigated. Concerning non-active reefing, two sets of measurements are presented in Figure 14b and Figure 14c for 20% and 5% skirt line ratios respectively. Examining 20% passive reefing in Figure 14b, steady-state drag area is reduced by 46% compared to its unreefed counterpart. Such a significant reducing in the drag area of a main DGB parachute is advantageous in sounding rocketry recovery for two key reasons. Primarily, the trajectory of a drogue parachute may be substituted with a reefed DGB configuration. In case the drag reduction achieved by reefing is not adequate, a drogue parachute may be required. Nevertheless, a reefed main parachute would significantly reduce the opening shock load. For example, a 5% reefed main parachute leads to an opening shock load of 29% as that of an unreefed parachute. This reduction in opening shock load is explained by Figure 14c, where the drag area is reduced by as much as 61%. Smaller opening shock loads lead to lighter structural designs of key bulkheads in sounding rockets.

Over and above that, the peak parachute opening load of the unreefed parachute in Figure 14a reaches a value

DOI: 10.13009/EUCASS2023-447

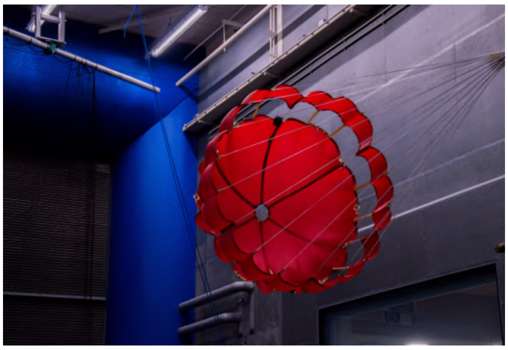

(a) Isometric view: skirt line detached

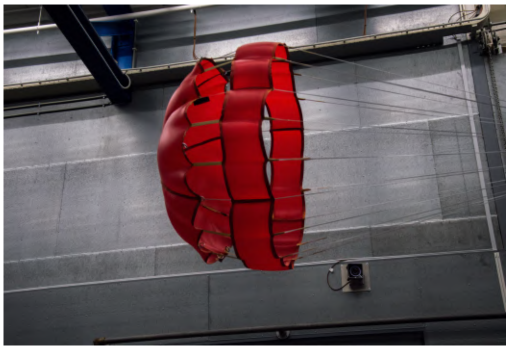

(b) Side view: canopy fully inflated

Figure 13: Disreefed DGB in OJF Windtunnel

64% larger than the steady-state drag at a freestream speed of 27 m/s. When compared to the ratio of peak-to-steady drag coefficient obtained by Underwood[19] of 2.07 for free-flight testing for a Huygens-like DGB parachute with a reference diameter 95% of that tested according to Table 4, the design of the present work has a more desirable performance. Remarkably, the opening load is reduced to a value 35% larger than the steady-state equivalent for 5% reefing and to 41% for 20% reefing.

The skirt reefing was successfully disreefed during the wind tunnel operations to demonstrate the reduction in opening loads as illustrated in Figure 14d. Contrary to the experience retrieved from the literature,[1,21] no violent instabilities or oscillations were observed. The stable behavior in conjunction with the improved aerodynamic performance indicates the suitability of skirt reefing for scaling DGB parachutes in the subsonic regime. The clear advantage of reefing is evident as it significantly decreases the opening loads and alleviates stress on the parachute materials. This reduction in stress may enable the scalability of parachutes to accommodate heavier payloads and sounding rockets.

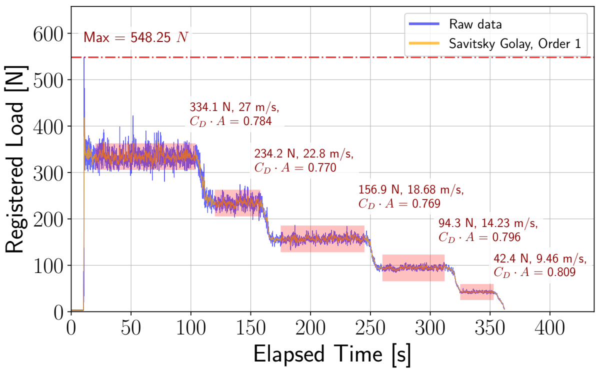

(a) Unreefed

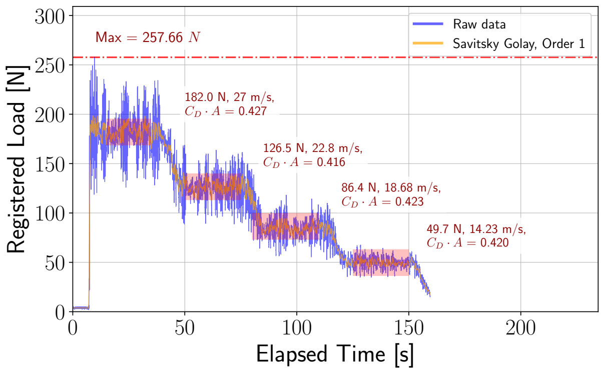

(b) 20% reefing applied, non-active

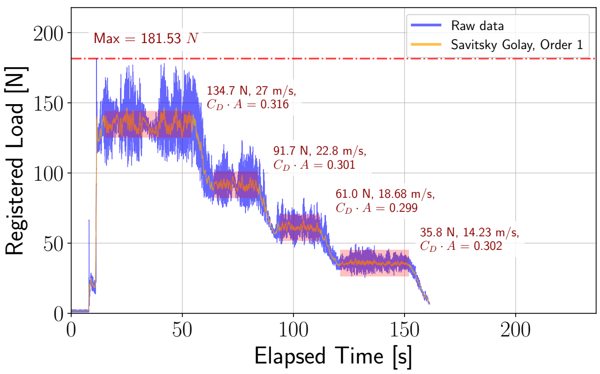

(c) 5% reefing applied, non-active

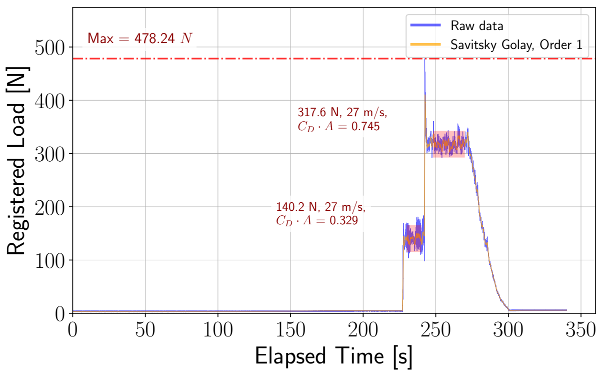

(d) 5% reefing applied, active

Figure 14: Load vs. time plots of performed wind tunnel tests. Average drag and drag coefficients labeled at select wind tunnel speeds

DOI: 10.13009/EUCASS2023-447

7. Conclusions and Recommendations

The work presented has addressed the development and testing of a novel Huygens-like DGB parachute with active skirt reefing. The design methodology and cost-effective manufacturing adopted provide insightful considerations on the scaling of DGBs for heavier payloads. Although skirt reefing is typically not recommended for DGBs in the literature due to violent instabilities,[1,21] the present work has successfully verified its suitability for subsonic deployment and inflation. The reduction in opening load factors, varying between 35% and 41% for 5% and 20% reefing respectively, demonstrates the effectiveness of the reefing strategy implemented. It is recommended to experiment with different disreefing techniques, exploring alternative methods to achieve desired deceleration characteristics. The steady-state drag performance of the parachute was tested in the OJF at near-laminar subsonic freestream conditions. The measured drag coefficient of 0.54-0.57 showed consistent agreement with the values retrieved from the literature.[8,20] It is suggested to include sensors capable of measuring the stability characteristics of the parachute, such as oscillation angles, through future experiments or simulations. These would provide valuable insights for design optimization. Exploring different scaling factors and assessing their impact on performance would also help tailor the reefed DGB design for various payload masses and deployment scenarios.

Another recommendation is concerned with the enhancement of the manufacturing strategy. The prototype DGB parachute has been successfully constructed using F111 nylon fabric, reinforced with aramid tape, connected to a riser using spliced Spectra 725 lbs suspension lines. An extensive tensile test campaign reveal key strength/stiffness insights pertinent to in-flight inflation and shock loads. Namely, knots lead to significantly more strength reduction than spliced line configurations. Therefore, the authors recommend splicing hollow-braided rope to fully extract the material properties of suspension lines. Should knots be deemed absolutely necessary, Poacher's knot was found to have the highest UTS. Concerning gore assembly, the use of reinforcement tape is necessary in regions of high stress concentrations. Aramid-based tape demonstrated marginally better performance than nylon alternatives. At the same time, no significant difference was established between zig-zag and straight stitches. Further work may entail aerothermal simulations to verify that the parachute can be safely operated in the desired flight regime. It is encouraged to perform high-fidelity structural analyses on the parachute to eliminate unnecessary canopy reinforcement or to use thinner fabrics/ropes. These results coupled with the recommendations of this paper aim to enhance the control, manufacturing reliability, stability, and scalability of reefed DGBs.

Acknowledgments

The authors acknowledge the members of the SPEAR II group at Delft Aerospace Rocket Engineering who directly and indirectly contributed to the research in this paper. They would also like to thank the Parachute Research Group and the Stratos V team from the Delft Aerospace Rocket Engineering student society for providing reference material and advice. They finally extend the acknowledgments to the Faculty of Aerospace Engineering at Delft University of Technology for generously granting access to the OJF wind tunnel and the Delft Aerospace Structures and Materials Laboratory.

References

[1] I. G. Clark, T. Rivellini, and M. Adler. Development and testing of a new family of low-density supersonic decelerators. *AIAA Aerodynamic Decelerator Systems Conference*, 2013.

[2] I. G. Clark and C. Tanner. A historical summary of the design, development, and analysis of the disk-gap-band parachute. *2017 IEEE Aerospace Conference*, pages 1–17, 2017.

[3] Delft University of Technology. Open Jet Facility, retrieved June 2023. `https://www.tudelft.nl/lr/organisatie/afdelingen/flow-physics-and-technology/facilities/low-speed-wind-tunnels/open-jet-facility`.

[4] E. G. Ewing. Ringsail parachute design. Air Force Flight Dynamics Laboratory TR 72-3, Northrop Corporation Ventura Division, 1971.

[5] J. Houmar. Stress analysis of the viking parachute. *4th Aerodynamic Deceleration Systems Conference*, 1973.

[6] T. W. Knacke. *Parachute Recovery Systems Design Manual*, 1985.

DOI: 10.13009/EUCASS2023-447

[7] M. Kobald, C. Schmierer, U. Fischer, K. Tomilin, and A. Petrarolo. A Record Flight of the Hybrid Sounding Rocket HEROS 3. *Transactions of the Japan Society For Aeronautical and Space Sciences, Aerospace Techncology Japan*, 16(3):312–317, 2018.

[8] J. S. Lingard, A. Saunders, J. C. Underwood, S. B. Rogers, J. Merrifield, and L. Ferracina. Supersonic parachute testing using a Maxus sounding rocket piggy-back payload. *24th AIAA Aerodynamic Decelerator Systems Technology Conference*, 2017.

[9] Seal Maker. Material data sheet f111-b85. https://sgpolimer.ru/upload/iblock/Sealmaker/NBR/FPM_F111-B85_black.pdf.

[10] M. Neal and P. Wellings. Design and qualification of the descent control sub-system for the Huygens probe. *13th Aerodynamic Decelerator Systems Technology Conference*, 1995.

[11] L. Pepermans, E. Menting, M. Rozemeijer, B. Koops, N. S. Dahl, N. Suard, S. Khurana, F. van Marion, F. Kuhnert, and M. Serman. Comparison of various parachute deployment systems for full rocket recovery of sounding rockets. In *7th European Conference for Aeronautics and Aerospace Sciences*, 2017.

[12] L. Pepermans, S. O. Scholts, E. Menting, T. Britting, A. L. Rivera, S. Dhiyaneeswaran, W.L. Toussaint, T. C. Bosboom, and B. Koops. Integration of the large envelope advanced parachute system in stratos iv. *Advances in Astronautics Science and Technology*, 5(4):295–308, 2022.

[13] J. Potvin and S. Patel. Simple Calculation of Skirt Reefing Line Tension on Low-Porosity Canopies Used at Very Small Reefing Ratios. *20th AIAA Aerodynamic Decelerator Systems Technology Conference*, 2009.

[14] J. S. Preisser and R. B. Grow. High-altitude flight test of a reefed 12.2-meter-diameter disk-gap-band parachute with deployment at a mach number of 2.58. NASA TN D-6469, National Aeronautics and Space Administration, 1971.

[15] A. Stamminger, M. Czech, H. Griebel, M. Hörschgen, O. Persson, M. Pinzer, J. Rießelmann, and A. Shavsavar. REXUS-4: Vehicle And Subsystems Design, Flight Performance and Experiments. In *19th ESA Symposium on European Rocket and Ballloon Programmes and Related Research*, pages 541–546. ESA Communication Production Office, 2009.

[16] Copenhagen Suborbitals. Nexo II, retrieved May 2023. https://copenhagensuborbitals.com/missions/nexo-ii/.

[17] J. C. Underwood. A system drop test of the Huygens Probe. *12th Lighter-Than-Air Systems Technology Conference*, 1997.

[18] J. C. Underwood, A. Saunders, S. B. Rogers, J. S. Lingard, L. Marraffa, and L. Ferracina. Subsonic Parachutes for Future Mars Missions. *8th European Symposium on Aerothermodynamics for Space Vehicles, Lisbon, Portugal*, 2015.

[19] J. C. Underwood, A. Saunders, S. B. Rogers, J. S. Lingard, L. Marraffa, L. Ferracina, G. L. Larose, and S. A. McTavish. Subsonic wind tunnel testing of various parachute types. *23rd AIAA Aerodynamic Decelerator Systems Technology Conference*, 2015.

[20] J. C. Underwood and R. J. Sinclair. Windtunnel testing of parachutes for the huygens probe. *The Aeronautical Journal*, 101(1008):357–364, 1997.

[21] A. Witkowski and M. Kandis. Reefing the Mars Science Laboratory parachute. *2010 IEEE Aerospace Conference*, 2010.

[22] Zwick Roell Group. Proline Technical Datasheet, 2014. https://www.zwickroell.com/products/static-materials-testing-machines/universal-testing-machines-for-static-applications/proline/.